

*Report to HQ. GRANT
IN-90-CR
98645
21P.*

FINAL TECHNICAL REPORT

for

NASA GRANT NAGW-550

"ORIGIN AND TRANSPORT OF HIGH ENERGY PARTICLES IN THE GALAXY"

March 1, 1984 - February 28, 1987

John P. Wefel
Associate Professor of Physics
Principal Investigator

Department of Physics and Astronomy
Louisiana State University
Baton Rouge, LA 70803-4001

submitted to

National Aeronautics and Space Administration

{NASA-CR-181368} ORIGIN AND TRANSPORT OF
HIGH ENERGY PARTICLES IN THE GALAXY Final
Technical Report, 1 Mar. 1984 - 28 Feb. 1987
(Louisiana State Univ.) 21 p Avail: NTIS
HC A02/MF A01

N87-30232

Unclas
0098645

CSCL 03B G3/90

"ORIGIN AND TRANSPORT OF HIGH ENERGY PARTICLES IN THE GALAXY"

Final Technical Report NAGW-550

I. INTRODUCTION:

NASA Grant NAGW-550 was established in 1984 at Louisiana State University to provide support for our research directed towards understanding the origin, confinement and transport of cosmic ray nuclei in the galaxy. The work involves new interpretations of the existing cosmic ray physics database derived from both balloon and satellite measurements, combined with an effort directed towards defining the next generation of instruments for the study of the cosmic radiation. In spring, 1987 a complete review of the Particle Astrophysics program was conducted by NASA Headquarters, and this resulted in the termination of NAGW-550 and its replacement by a new grant (NAGW-1027) under which we will both extend the work performed under NAGW-550 and initiate a new project involving new experimental measurements. Thus, the work supported by NASA under this grant has led to significant new research results from the interpretation of existing data and has provided the basis from which to plan new experimental programs.

II. PROJECT OVERVIEW:

Cosmic rays are the only sample of matter accessible to experimental investigation that has its origin outside of our solar system. Over the last 15 years, improvements in satellite and balloon instrumentation have lead to (1) highly accurate measurements of elemental abundances up to $Z = 30$ over a wide range of energies, (2) even- Z element abundances for $Z > 30$ (UH) nuclei, and (3) isotopic composition measurements for the major elements up to silicon. In the near future, this impressive dataset will be extended to additional energies, and isotopic measurements will be made for additional elements. For some elements and isotopes the cosmic ray abundance is now known to a greater degree of accuracy than the corresponding solar or galactic abundance.

What is needed, however, is a systematic interpretation of the available data, taking into account all known energy-dependent processes and realistically assessing the uncertainties in the interpretation. For the past three years, this has been the major research effort supported by this grant.

Of ultimate interest are the nature of the matter at the cosmic ray source(s) and the transport of these high energy nuclei through the interstellar medium. It is necessary to understand both the confinement of, and the matter traversed by, the cosmic rays in order to unfold the measured composition and correct for secondary particle production in the interstellar medium. This is critical for investigating the elemental and isotopic composition in the source region. It is the source ratios that provide clues to the nature of the nucleosynthesis that formed cosmic ray matter and thereby a measure of the extent of chemical evolution in the galaxy.

A major part of solving this general problem resides in detailed calculations of the propagation of charged particles in the galaxy. The current database shows that the propagation must be done in an energy dependent manner taking into account all of the energy dependence of the input parameters, most notably cross sections, with the goal to reproduce the behavior, as a function of energy, of the cosmic ray measurements.

During this grant, we have studied both the shape and the energy dependence of the cosmic ray pathlength distribution in the galaxy, demonstrating that the simple "leaky box" model is not a good representation of the detailed particle transport over the energy range covered by the database. Further, we have investigated alternative confinement models, have analyzed the confinement lifetime in these models based upon the available data for radioactive secondary isotopes, have studied the source abundances of several isotopes using compiled nuclear physics data and the detailed transport calculations and have begun to investigate the effects of distributed particle acceleration on the secondary to primary ratios.

This approach grew out of a program originally begun at the University of Chicago in the research group headed by Prof. J. A. Simpson and has continued, in part, as a collaborative venture between Chicago and our group at LSU. In addition, we have worked, in part, with researchers at LBL and at Boston University. Such collaborations allowed more resources to be applied to the problems than could be generated under this grant by the LSU group alone.

The second aspect of this research program involved investigations of new experimental opportunities and planning for future NASA projects. In this area we participated in the Science Steering Committee for the Heavy Nuclei Collector Facility originally planned for launch as part of the LDEF program, organized a Workshop on "Cosmic Ray and High Energy Gamma Ray Experiments for the Space Station Era" and published the proceedings of the meeting, provided input to the TUFUSS subcommittee on Astrophysics Investigations for the Space Station and were selected to participate in the definition of the Astromag Facility for the Space Station. This latter activity will be continuing for the next several years.

III. SUMMARY OF RESULTS:

A. The Pathlength Distribution

A central focus of our research has been, and continues to be, the pathlength distribution (PLD) followed by the cosmic ray particles in their transport from the source regions to the Earth. The PLD contains the details of the history of the cosmic rays in terms of the matter traversal and encompasses, as the measurable parameter, the predictions of different models for the confinement and propagation of the cosmic rays.

Figure 1 demonstrates the dual problem posed by the experimental results. Shown are compilations of experimental data for the B/C and sub-Fe/Fe ratios, both predominately secondary to primary ratios, as a function of energy. Superposed are curves giving the results of energy independent propagation calculations for exponential PLD's whose means (in g/cm^2) are indicated by the numbers attached to each curve. The experimental data

indicate an energy dependence to the ratios extending from the lowest to the highest available energies. Clearly, the calculations must be energy dependent in order to reproduce the measurements over the full energy range.

The second feature to note about Figure 1 is that in any energy interval below several GeV/nucleon, the curve that fits the B/C ratio does not simultaneously reproduce the sub-Fe/Fe ratio. Thus, there is a charge dependence in the propagation which means that the shape of the PLD must be different from a pure exponential, which is the PLD implied by the leaky-box model.

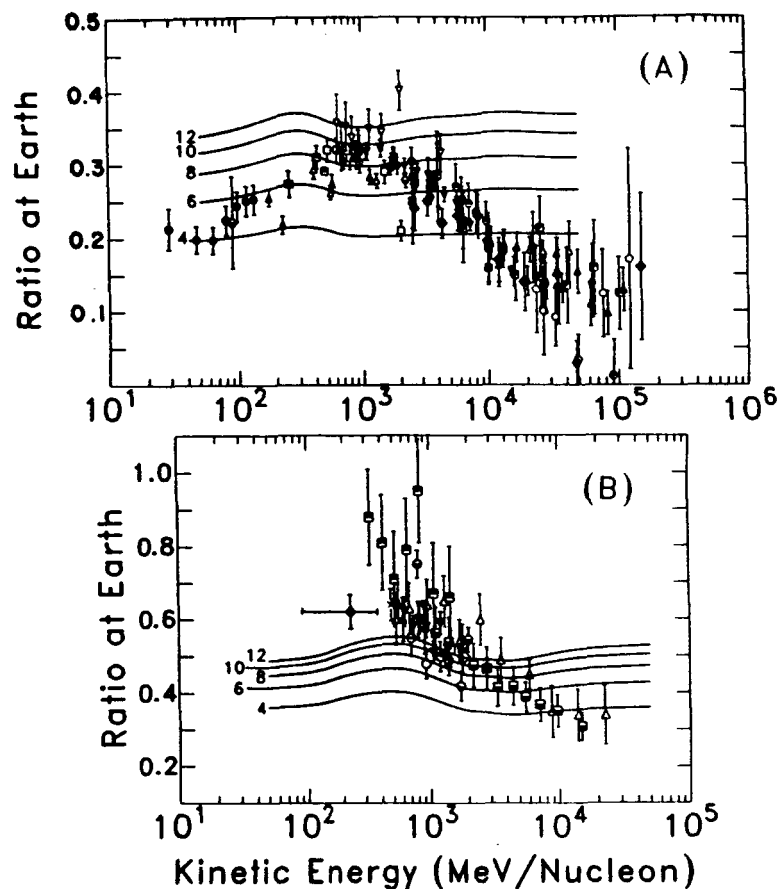


Figure 1: Compiled measurements of (A) the B/C and (B) the sub-Fe/Fe ratios as a function of energy compared to the results of energy independent propagation calculation for exponential PLD's with mean values given by the numbers next to the curves.

To analyze this data quantitatively we have developed a detailed propagation code for particle transport in the galaxy and coupled the results to a full solar modulation calculation for particle transport in the Heliosphere. The details of the calculation are described in Garcia-Munoz et al., 1987. Here we will cite only a few of the parameters which must be included accurately in the calculations. Figure 2 shows, again, the B/C and sub-Fe/Fe data compared to calculations using energy independent exponential PLD's both including ionization energy loss, curves (a), and neglecting ionization, curves (b). The effect of ionization energy loss on the calculated ratios is dramatic at low energies and is appreciable to beyond 5-6 GeV/nucleon.

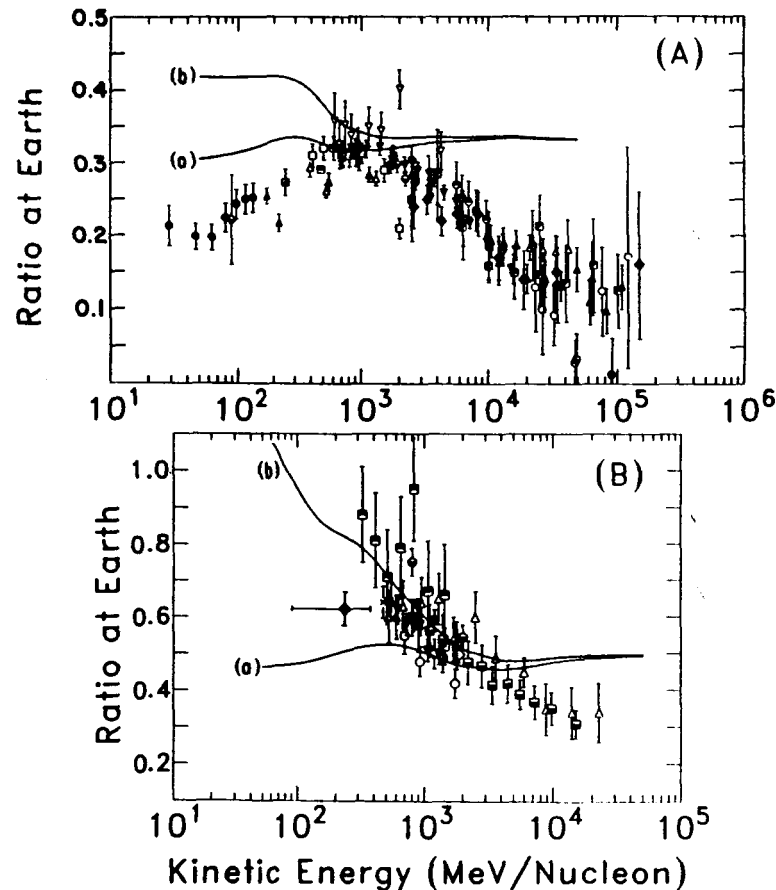


Figure 2: Compiled measurements of (A) the B/C and (B) the sub-Fe/Fe ratios as a function of energy compared to the results of energy independent galactic propagation calculations plus solar modulation. The exponential PLD has a mean of 9.25 g/cm^2 . Curves (a) show the results including ionization energy loss and curves (b) the results without energy loss.

Figure 3 gives for B/C a comparison of the calculated curves for different levels of solar modulation. The solar modulation level is not a free parameter in the calculations, but must be fixed by the level of solar activity existing at the time the measurements were performed. Most of the data on Figures 1-3 were obtained during the last solar minimum period 1974-1978 for which the solar activity level was reasonably constant. The modulation during this period corresponds to $\phi = 245 \text{ MeV/nucleon}$ which was adopted for the PLD analysis.

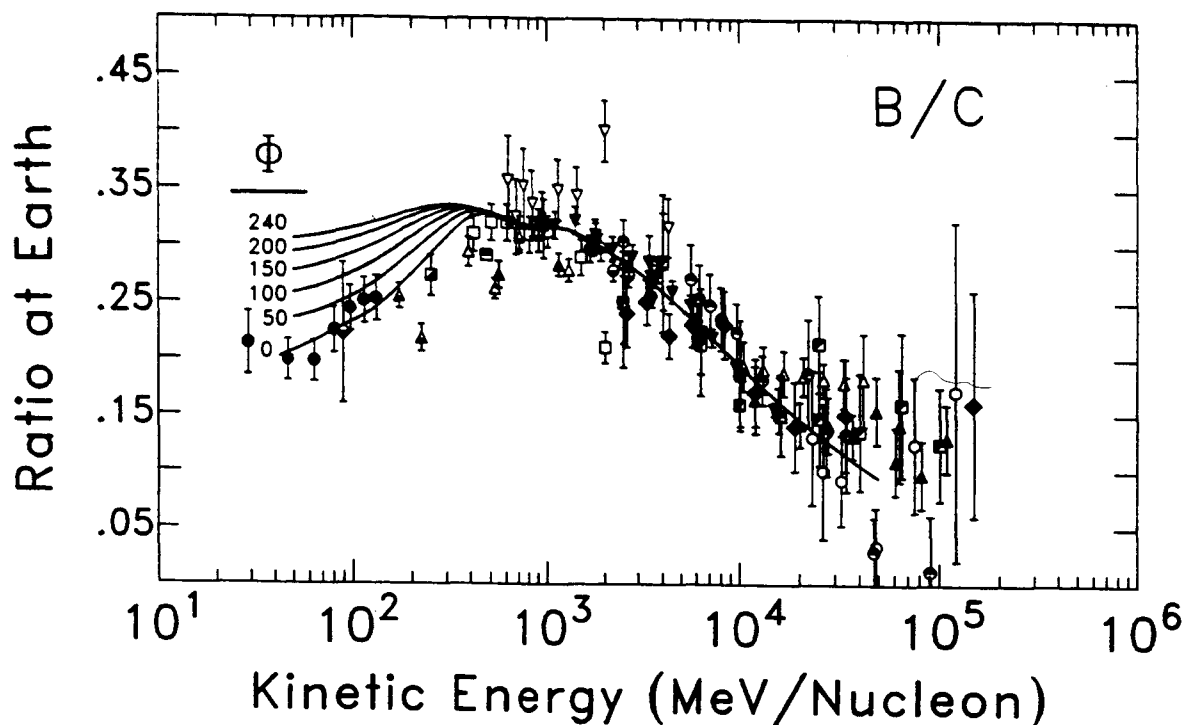


Figure 3: Compiled data on the B/C ratio compared to calculations for varying levels of Solar Modulation. The parameter Φ gives the level of modulation in terms of the adiabatic deceleration in MeV/nucleon experienced by a particle with $A/Z = 2.0$.

Assuming a purely exponential PLD and including all of the known energy dependences in the input parameters to the calculation, we have determined the energy dependence of the mean of the exponential PLD needed to reproduce the experimental data on the B/C ratio. The result is shown in Figure 4 in which the solid curve in the upper panel is the result of this analysis. The dotted and dashed curves show the uncertainty limits corresponding, respectively, to uncertainties in the fragmentation cross sections and to uncertainties in both the cross sections and the experimental B/C measurements. The dashed limits are reproduced as the shaded region in the lower portion of the figure and compared to theoretical calculations for the dynamical halo model with a galactic wind characterized by velocities of: (1) 9 km/s and (2) 17 km/s. The experimentally determined PLD mean shows a stronger energy dependence than either of the theoretical curves which, in a dynamical halo model, implies galactic wind velocities in excess of 25 km/s — and possibly much larger.

The conclusion from Figure 4 is that the PLD must be energy dependent both at low and high energies. This implies that cosmic ray confinement and transport in the galaxy is an inherently energy dependent process and thereby opens up a new dimension to the problem for theoretical analysis.

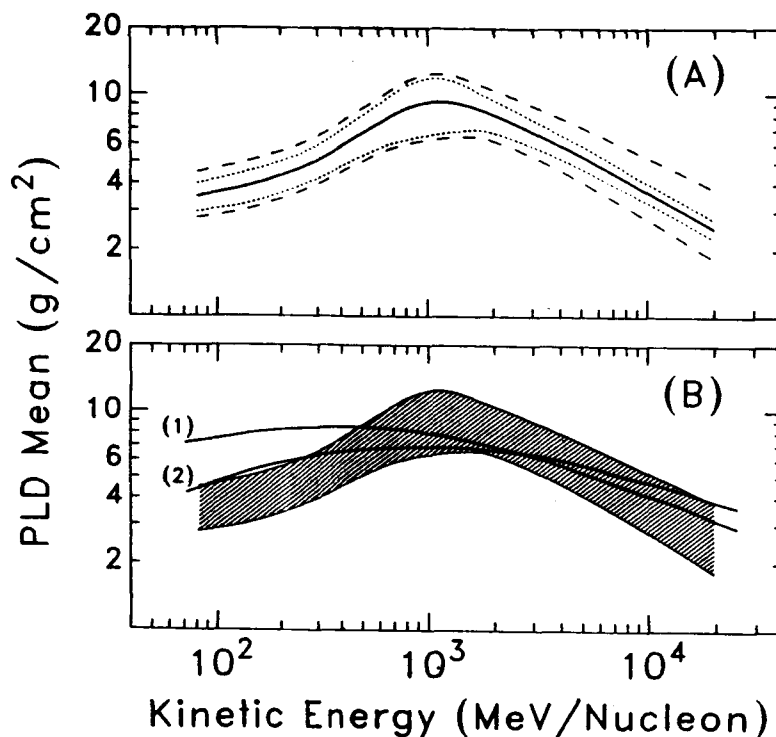


Figure 4: The mean value of an exponential PLD as a function of energy required to fit the B/C measurements. In (A) the solid line shows the energy dependence of the mean with the dotted lines giving the uncertainty due to the nuclear fragmentation cross sections. The dashed lines show the uncertainty obtained by including the errors in the B/C measurements as well. In (B) the shaded region corresponds to the limits from the dashed curves of part (A), and this band is compared to curves from the dynamical halo model for two galactic wind velocities.

The next step in the analysis was to apply this energy dependent exponential PLD to calculate other secondary to primary ratios. The result for B/C and sub-Fe/Fe is shown in Figure 5. Note that the calculated curve which fits the B/C ratio does not reproduce the sub-Fe/Fe ratio at low energies. The calculations fall below the data, indicating that more fragmentation of iron nuclei is required. Since the interaction cross section for iron is about three times the interaction cross section for carbon, the sub-Fe/Fe ratio is sensitive to smaller pathlengths in the PLD than is the B/C ratio. Thus, one means to obtain additional iron fragmentation with only a small effect on the B/C ratio is to modify the shape of the PLD by truncation, or the removal of short pathlengths. This is illustrated in Figure 6 which shows three PLD's. The top plot shows a pure exponential PLD which contains a large proportion of paths characterized by small values of X (g/cm^2). Truncating such a distribution involves removing some of the short

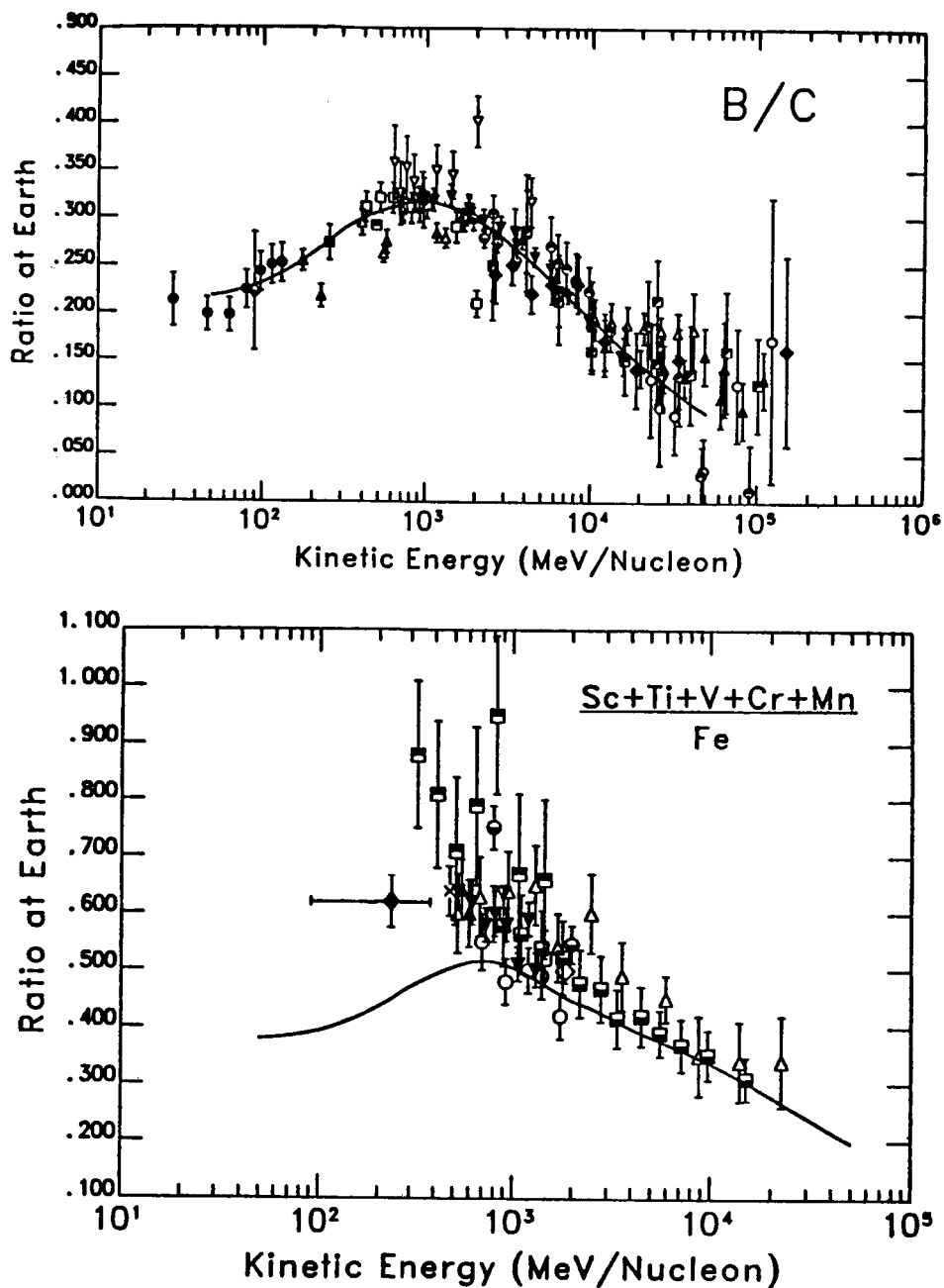


Figure 5: Compiled data for B/C and sub-Fe/Fe ratios compared to the results from the energy dependent exponential PLD shown in Figure 4.

paths such as is done in part (B) where all particles are required to pass through a minimum amount of material or in part (C) where the removal is done more gradually. In both (B) and (C), the PLD is characterized by two parameters, a mean for the exponential part and a second parameter describing the depletion of short pathlengths.

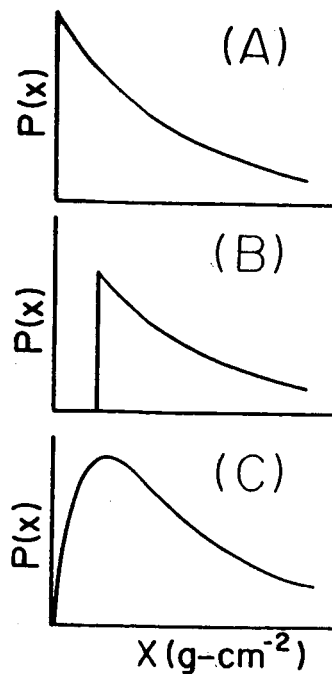


Figure 6: Schematic illustration of three PLD's: (A) Exponential PLD, (B) Zero-short PLD, (C) Double exponential PLD.

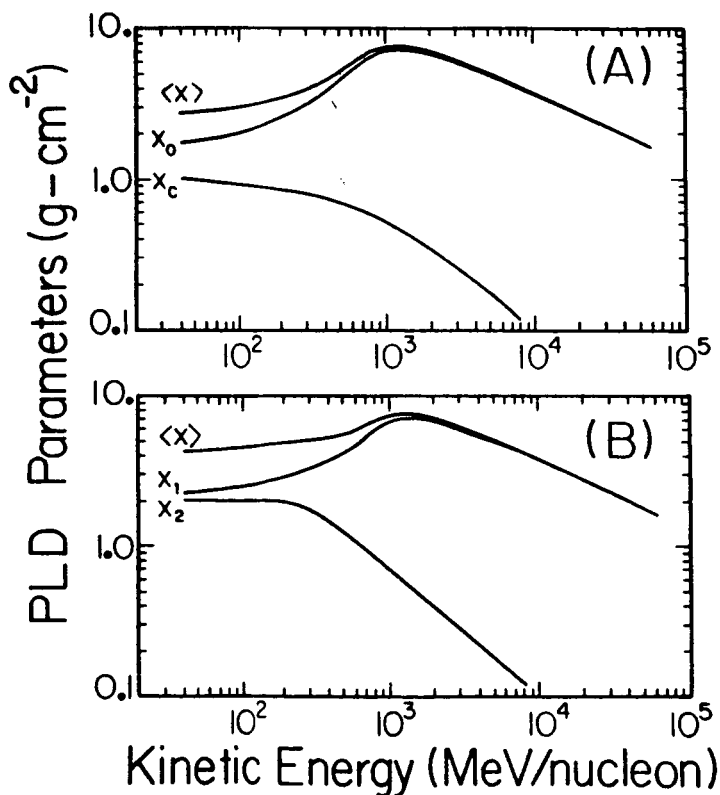


Figure 7: Energy dependence of the parameters in (A) the Zero-short PLD of Figure 6B and (B) the Double-exponential PLD of Figure 6C. Parameters x_0 and x_1 represent the mean of the exponential part of the distribution while parameters x_c and x_2 define the truncation. The mean $\langle x \rangle$ of the PLD is indicated in both cases.

A closer look at the lower part of Figure 5 indicates that the curve is in moderately good agreement with the experimental sub-Fe/Fe ratio at high energies, but the curve lies progressively farther from the data as the energy is decreased. Thus, this behavior indicates that the truncation of the PLD must itself be energy dependent.

The remaining task is to determine if a PLD such (B) or (C) in Figure 6 can reproduce simultaneously the measured B/C and sub-Fe/Fe ratios and to determine the energy dependence of the two parameters in the PLD. The results from such an analysis are shown on Figure 7 with the top panel corresponding to the zero-short PLD of Figure 6B and the lower panel corresponding to the Double-exponential PLD of Figure 6C. The parameters X_0 and X_1 correspond to the mean of the exponential part of the distribution and are found to have essentially the same energy dependence as was found in Figure 4 for the case of a pure exponential. What is new here is the energy dependence of the truncation parameters (X_0 or X_2) which are largest at low energies and decrease in importance with increasing energy. For both PLD's the energy dependence of the mean amount of material traversed is indicated.

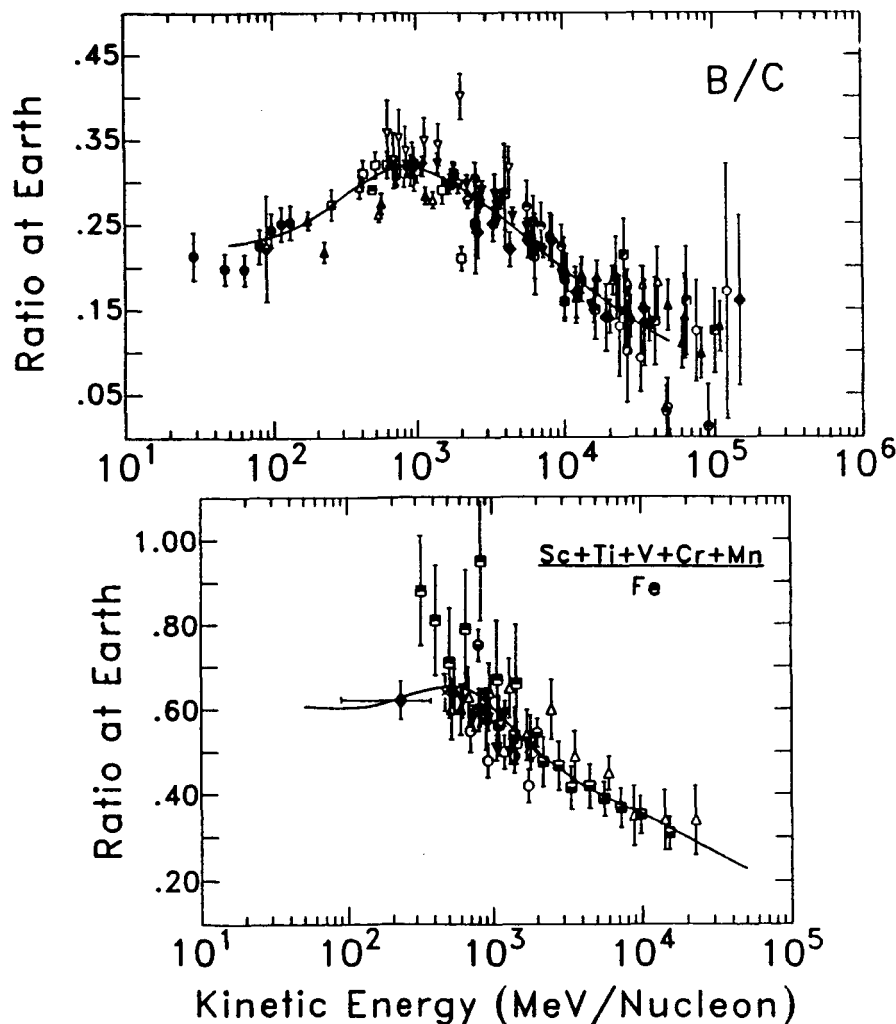


Figure 8: The results of propagation calculations for the Zero-short, truncated exponential PLD compared to the B/C and sub-Fe/Fe measurements.

The final fit, using the zero-short parameters on Figure 7, to the B/C and sub-Fe/Fe ratios is illustrated in Figure 8 and is applied to other ratios in Figure 9. For Li/C and Be/C the experimental data are significantly inferior to the B/C measurements, and additional experimental work remains to be done. However, the calculations do reproduce the best of the measurements adequately. The N/O ratio in Figure 9 is not strictly a secondary to primary ratio since there is an important source component of ^{14}N . Modifying this source component has the effect of shifting the calculated curve up or down. Thus, the N/O ratio provides a test for the shape of the calculated results rather than for their absolute normalization, and the present results do reproduce the shape of the N/O data as a function of energy quite well.

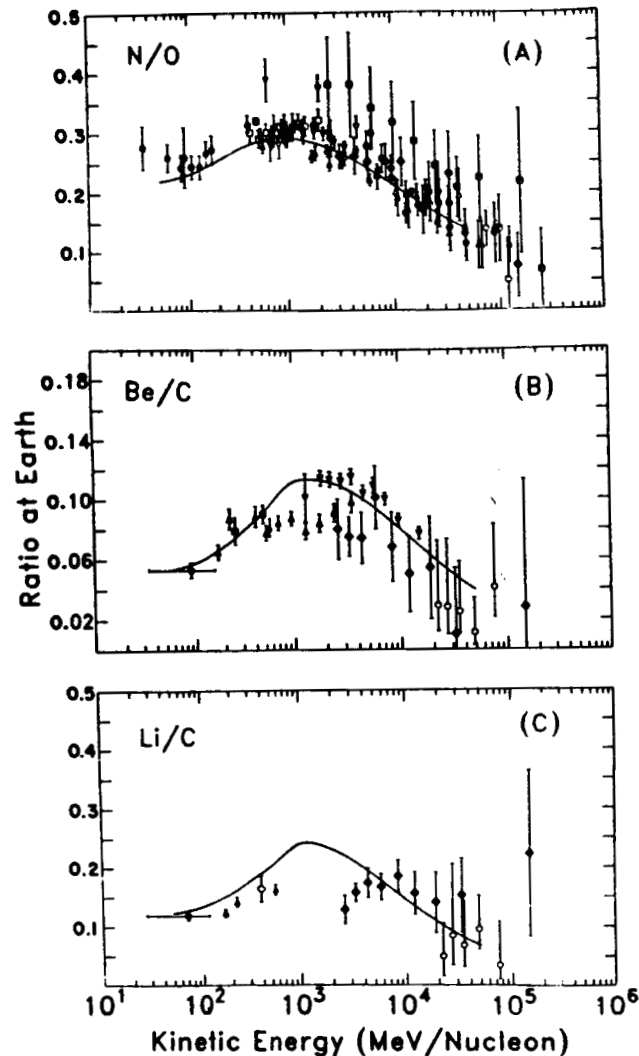


Figure 9: Comparison of the calculated ratios using the truncated zero-short PLD of Figures 7 and 8 to compiled experimental data for (A) the N/O, (B) the Be/C and (C) the Li/C ratios.

The empirical PLD's of Figure 7 can be interpreted in terms of models for cosmic ray confinement and escape. The zero-short PLD (Figures 6B and 7A) could represent a shell of matter around the cosmic ray source regions from which the particles escape, in an energy dependent fashion, into the larger galactic volume in which their confinement and escape is also energy

dependent. A similar interpretation can be made for the double-exponential PLD (Figures 6C, 7B). The important point here is that the interpretation involves two confinement regions. Determining the nature of these regions and the physical processes operating in them remains a significant challenge for future research.

B. The Confinement Regions

One technique for studying the confinement of the cosmic rays is to use the decay of a long-lived, secondary isotope as a tracer of the density experienced by the cosmic rays during their confinement and transport. Most successful of these has been the isotope ^{10}Be but other species, e.g. ^{26}Al , ^{36}Cl , can also be employed.

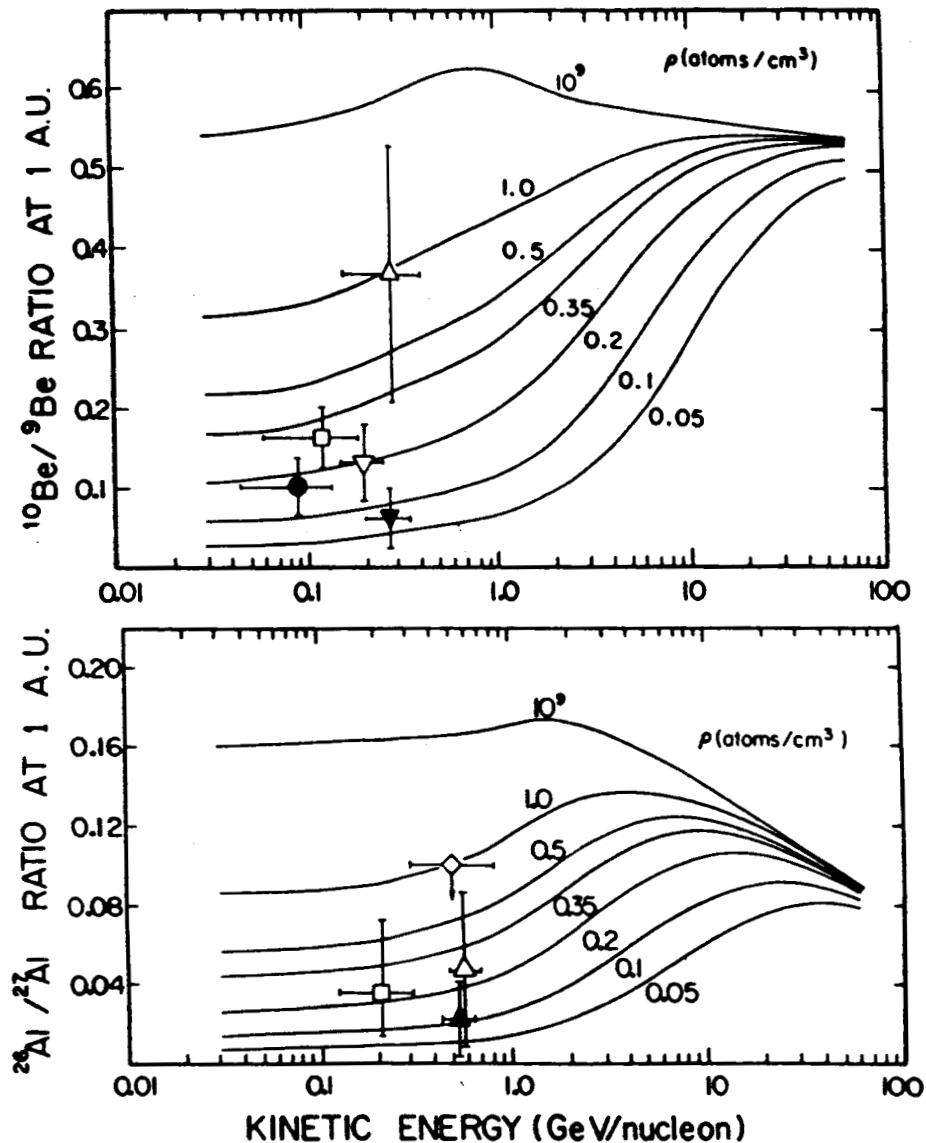


Figure 10: Compiled measurements of the $^{10}\text{Be}/^9\text{Be}$ (top) and $^{26}\text{Al}/^{27}\text{Al}$ (bottom) ratios compared to single region propagation calculations for a variety of matter densities in the confinement region.

Under this grant we have investigated the nature of the confinement regions using the two component propagation models described in the previous section. The calculations proceeded as follows. The propagation was performed for the first region, characterized by the parameters X_c or X_2 in Figure 7, for a variety of assumed densities. These results were then used as input to a second propagation calculation corresponding to the part of the problem characterized by parameters X_o or X_1 in Figure 7. This two stage approach allowed the effects of the different regions to be extracted.

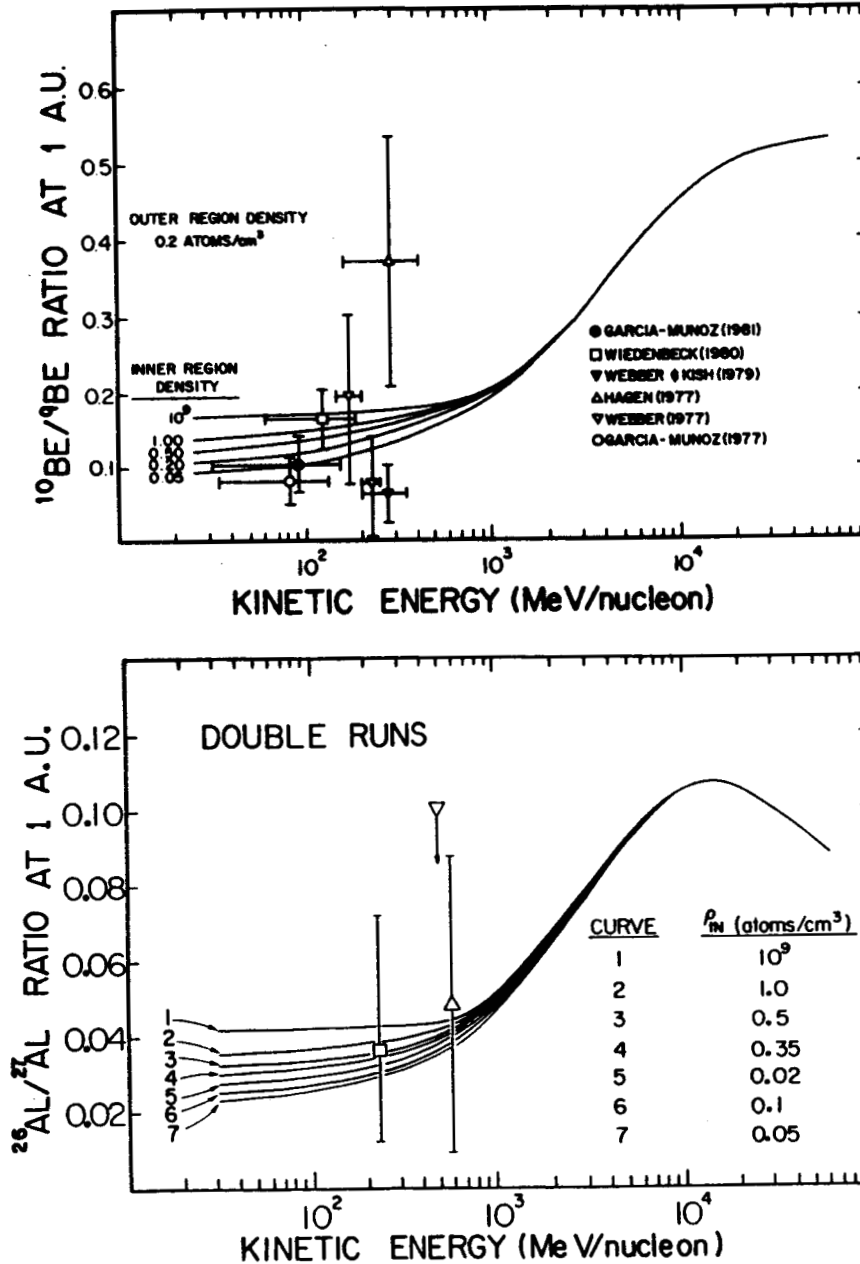


Figure 11: Calculated curves for double runs. In both cases the second ("outer") region had a density of 0.2 atoms/cm³ while the density in the first ("inner") region was allowed to vary.

Figure 10 shows the results for the standard case of a single confinement region for the species ^{10}Be and ^{26}Al . The experimental data are still of limited precision, but do indicate a rather low mean density in the

confinement volume, ~ 0.2 atoms/cm³. In the two confinement region model we would expect to see differences at low energies, since it is the parameters X_1 and X_2 which describe the additional confinement. Adopting a single value of 0.2 atoms/cm³ for the second part of the calculation, the results for various densities in the "inner" region are displayed in Figure 11. The single curves in Figure 10 are split into many curves depending upon the assumed density in the first (inner) region in the calculation.

The first conclusion to emerge for Figure 11 is that the densities in each region can be determined from a single isotope ratio provided accurate measurements are made at several energies. Measurements at ~ 100 MeV/nucleon are sensitive to the density in the inner region while measurements at > 1 GeV/nucleon sample the outer region. The level of precision needed for the isotope ratios is on the order of a few percent, considerably more accurate than current experimental results.

Figure 11 also shows that the density in the inner region can affect the interpretation of the data in terms of the mean density experienced during galactic propagation. For the current $^{10}\text{Be}/^9\text{Be}$ measurements the limiting cases have been evaluated, and Figure 12 displays some of the results. Curves A and B show the extremes in the assumed density for the inner region for a constant outer volume density of 0.2 atoms/cm³. Curves C and D show the extremes allowed for the density in the outer region by assuming limiting values for the inner region. Within the range of the current experimental data, the outer (galactic) confinement volume may have a density as low as ~ 0.1 atoms/cm³ and as high as 0.5 atoms/cm³. In the first case, it is necessary to invoke significant confinement in the low density, hot regions of the interstellar medium or in a galactic halo. For a mean density of ~ 0.5 atoms/cm³, significant halo confinement is not a necessity. Thus, the question of the densities in the confinement volumes in the two-region analysis is an important one since it involves the degree of participation of a galactic halo in the transport of cosmic rays. Improved experimental data, not only for ^{10}Be but also for ^{26}Al and ^{36}Cl , is required to answer this important question.

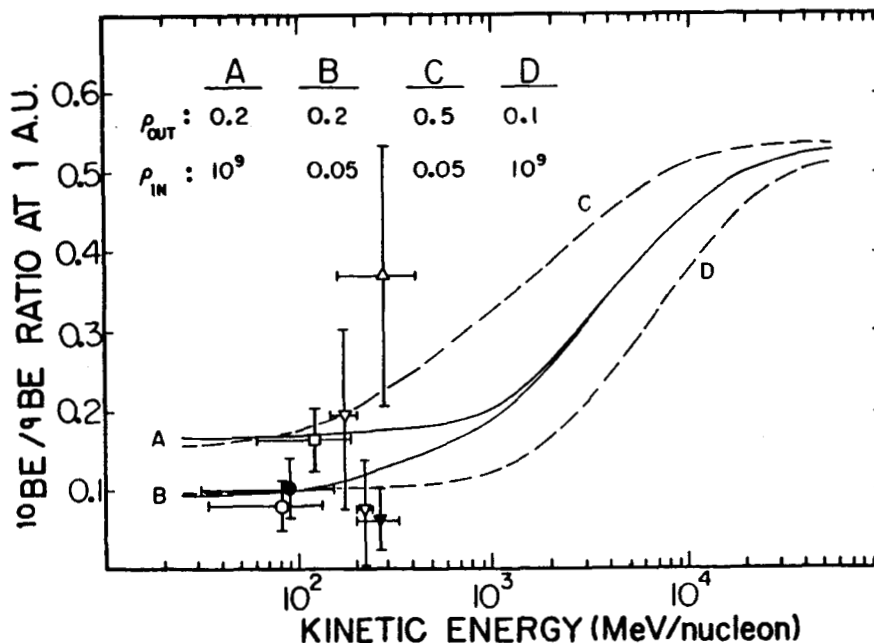


Figure 12: Experimental results for the ratio $^{10}\text{Be}/^9\text{Be}$ compared to limiting cases for the densities in the inner and outer confinement volumes.

C. Source Abundances

One of the ultimate goals of this research is to determine the elemental and isotopic ratios in cosmic ray source material as clues to the nucleosynthetic history of this sample of matter. In this area we have completed an analysis of the isotopic ratios of $^{14,15}\text{N}$ and $^{12,13}\text{C}$ in the cosmic ray source using several different forms for the (largely unmeasured) nuclear excitation functions, based upon different assumptions regarding the nuclear systematics. This latter involved compiling cross section measurements from the literature, comparing them to the results from semiempirical formulae and determining the excitation function to employ in the propagation calculations. An example of this is shown in Figure 13 for the reaction $^{16}\text{O} + p \rightarrow ^{13}\text{C}$ (+ progenitors). This excitation function is largely unmeasured, as a function of energy, and the LBL point at 2 GeV/nucleon was the only point available when this analysis was begun. The solid curve shows the excitation function given by the semiempirical formulae and the dot-dash curve represents this function scaled to agree with the LBL value. The dashed curve, however, shows a completely different behavior as a function of energy. This curve was derived from a fit to "equivalent" reaction channels, $^{12}\text{C} + p \rightarrow ^{10}\text{Be}$ and $^{13}\text{C} + p \rightarrow ^{10}\text{Be}$, whose measured cross sections are shown in the lower part of the figure.

Using the energy dependent propagation model described above, calculations were performed for each of the three excitation functions shown in Figure 13. The goal here is to relate the $^{13}\text{C}/\text{C}$ ratio measured at Earth to this $^{13}\text{C}/\text{C}$ ratio existing in the cosmic ray source regions. Figure 14 shows the correspondence with the three curves keyed to the curves on the top portion of Figure 13. The experimental data is shown as the solid horizontal line with the 1 σ uncertainty limits indicated. The arrows indicate $^{13}\text{C}/\text{C}$ ratios measured in the interstellar medium, GC and GR, or in the solar system, SS. For the 1 σ limits the source ratio can be anywhere between 0 and 2.5%. The experimental nuclear physics data at low energies for ^{13}C production (compiled on Figure 13) now indicates that the dashed excitation function should be eliminated from consideration, with an excitation function between the solid and dot-dash curves as the best current guess. In this case, the cosmic ray source ratio is constrained to the range ~0.5 - 1.5%. Such values are consistent with material of solar system composition or matter in the galactic ring but not with material from the inner regions of the galaxy near the galactic center.

Strengthening these conclusions requires advances on two experimental "fronts." First, the nuclear excitation functions must be determined more precisely than the data shown in Figure 13. Secondly, the uncertainties on the cosmic ray measurements must be reduced. Both types of improvements will be necessary in order to determine, precisely, the $^{13}\text{C}/\text{C}$ ratio at the cosmic ray source.

A similar analysis was performed for the nitrogen isotopes using the $^{12}\text{C} + ^{10,11}\text{B}$ reaction as a template for the nuclear excitation function. In this case the nuclear physics data still does not allow a clear choice of excitation functions and thereby limits the astrophysical interpretation of the cosmic ray data.

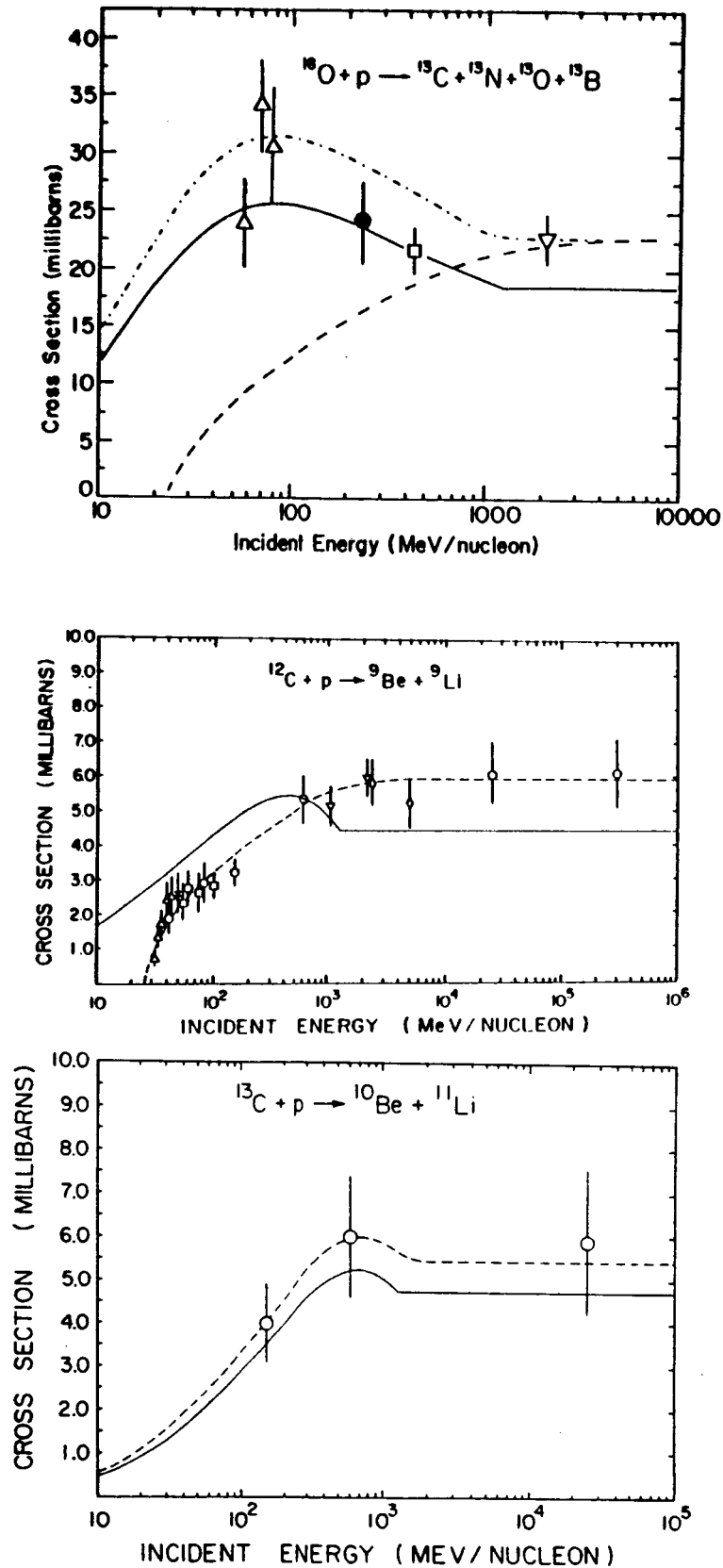


Figure 13. Nuclear Excitation Functions for (p, 3pn) reactions showing $^{16}\text{O} + ^{13}\text{C}$ (top), $^{12}\text{C} + \text{Be}$ (center) and $^{13}\text{C} + ^{10}\text{Be}$ (bottom). The lower two plots were used as a template to determine the dashed curve on the top plot.

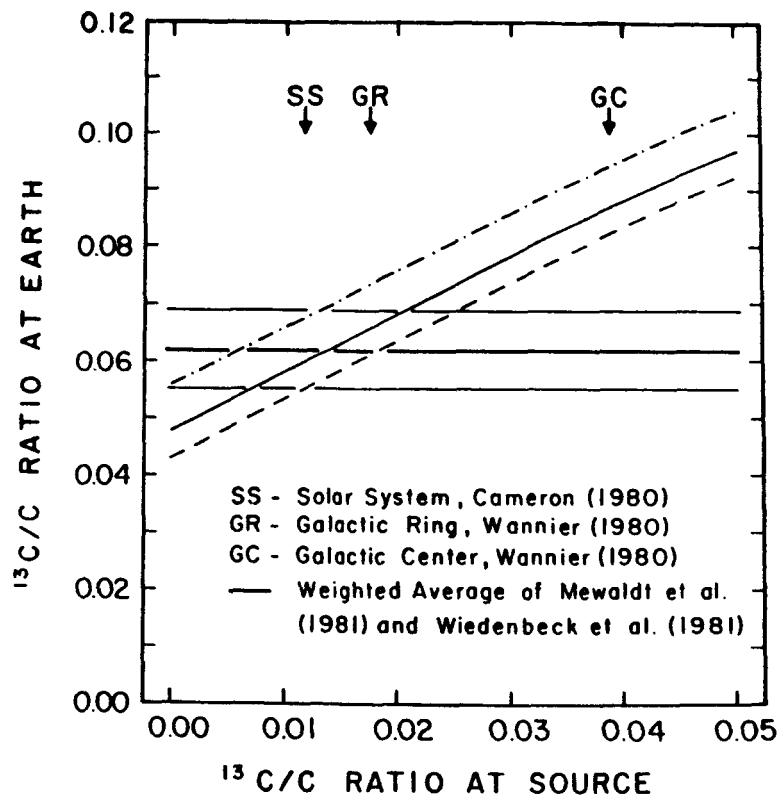


Figure 14. The ratio $^{13}\text{C}/\text{C}$ measured at Earth as a function of the $^{13}\text{C}/\text{C}$ ratio at the cosmic ray source. The results of the propagation calculations are shown as the three curves keyed to the nuclear excitation functions in Figure 13.

D. Distributed Reacceleration

One of the assumptions inherent in the cosmic ray propagation models that have been employed to date (and in the calculations described above) is the idea that the cosmic rays are accelerated once in or near the source regions and then propagate in the confinement region experiencing only energy loss processes. With the realization that shock waves can accelerate particles efficiently and that there are a large number of shock waves present at any one time in the interstellar medium, it is conceivable that the cosmic ray beam may encounter a number of shock waves with the effect of a net energy gain for the particles. This reacceleration has been invoked as a possible explanation for the energy dependence of the PLD, the depletion of short pathlengths and the apparent energy dependence in some of the measured isotope ratios. However, detailed model calculations are still lacking, especially at low energies.

Under this grant we initiated a new program to assess the probable effects of distributed reacceleration on the secondary to primary ratios and, thereby, the modifications which may be required in the models for confinement and transport of the cosmic ray particles. Theoretical calculations show that when a delta-function energy spectrum is subjected to shock acceleration a power law spectrum in momentum is obtained. Thus, shock acceleration can be described by a parameter giving the spectral index of the momentum power law. One additional parameter is needed to specify the number of times the cosmic

rays encounter shock waves. Clearly, both of these parameters are probably best represented by distribution functions, but for initial calculations fixed values of the parameters were employed.

The propagation code was first modified to include the energy redistribution implied by the distributed reacceleration model and was then run for a variety of shock spectral indices and frequencies of shock encounters, holding all of the other parameters in the calculation at their "standard" values as described previously — in particular an energy dependent PLD which fits the measured B/C data. Preliminary results for one such run are shown in Figure 15 for a shock spectral index of -4.5 , corresponding to medium strength shock waves. Curve (A) shows the standard case with no reacceleration while curves (B) - (E) show the effect of increasing the frequency of shock encounters. As expected, the reacceleration shifts the peak in the ratio to higher energies with increasing frequency of reacceleration events and modifies the energy dependence in the calculated ratio.

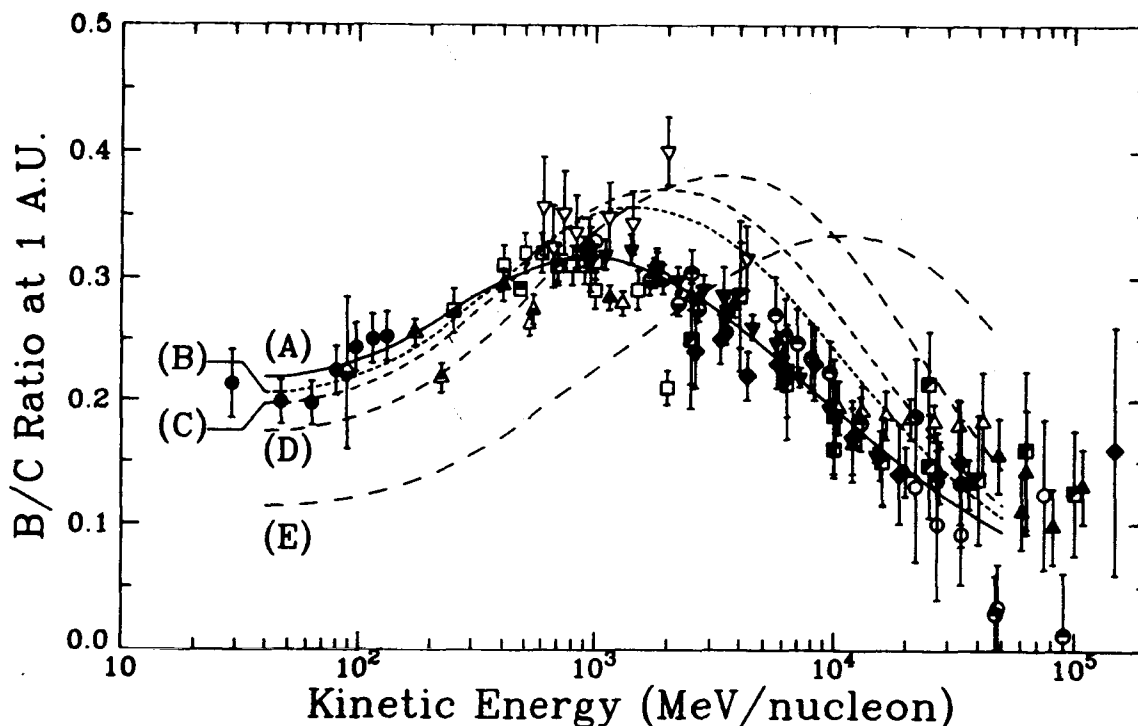


Figure 15. Compiled measurements of the B/C ratio compared to calculations invoking distributed reacceleration. Curve (A) is the fit to the B/C data from the energy dependent PLD shown in Figure 5. Curves (B) - (E) involve reacceleration for a shock spectral index of -4.5 and shock frequencies parameterized as (B) = 10, (C) = 6, (D) = 3, (E) = 1 where 10 corresponds to infrequent encounters and 1 corresponds to many reacceleration events.

None of the curves (B) - (E) actually reproduces the measured B/C data. This is because the PLD energy dependence was selected for the case of no reacceleration. What must be done next is to modify the energy dependence of the parameters in the PLD to force these reacceleration calculations to reproduce the experimental data. This will change both the mean pathlength at, for example, 1 GeV/nucleon and the energy dependence both above and below

1 GeV/nucleon. Since these energy dependences are the key to understanding the confinement and propagation process (as discussed previously), changes in these parameters imply modifications in the astrophysical models for cosmic ray confinement and transport.

The results on Figure 15 show that frequent encounters with reaccelerating shock waves, such as curve (E) are not likely. This is based upon the energy dependence of curve (E) compared to the experimental data. The modifications to the PLD parameters in this case will be excessive (if a suitable form can be found at all) and will probably not be astrophysically reasonable. For the other curves (B) - (D), the acceptability of the derived PLD's requires further study.

Following the derivation of the PLD parameters, the calculations must be applied to other secondary to primary ratios. This is the outline of the program of research in which we are presently engaged under the continuation of this research through NASA grant NAGW-1027.

IV. BIBLIOGRAPHY

A) Publications, Proceedings and Papers:

"The Pathlength Distribution for Galactic Cosmic Ray Propagation: An Energy Dependent Depletion of Short Pathlengths," M. G. Munoz, T. G. Guzik, J. A. Simpson and J. P. Wefel, *Astrophysical J. Letters*, 280, L13 (1984).

"Nuclear Fragmentation Cross Sections and Cosmic Ray Source Abundances," T. G. Guzik and J. P. Wefel, *Advances in Space Research*, 4, 93 (1984).

"The Cosmic Ray Pathlength Distribution at Low Energy: A New Probe of the Source/Acceleration Regions," T. G. Guzik and J. P. Wefel, *Advances in Space Research*, 4, 215 (1984).

"Galactic Propagation Models Consistent with the Cosmic Ray Lifetime Derived from ^{10}Be Measurements," T. G. Guzik, J. P. Wefel, M. Garcia-Munoz and J. A. Simpson, 19th ICR Conference Papers, (Washington, DC, 1985, National Aeronautics and Space Administration), Vol. 2, p. 76.

"Implications of New Measurements of $^{16}\text{O} + p + ^{12,13}\text{C}, ^{14,15}\text{N}$ for the Abundances of C, N. Isotopes at the Cosmic Ray Source," T. G. Guzik, J. P. Wefel, H. J. Crawford, D. E. Grenier, P. J. Lindstrom, W. Schimmerling and T. J. M. Symons, 19th ICR Conference Papers, (Washington, DC, 1985, National Aeronautics and Space Administration), Vol. 2, p. 80.

"Cosmic Ray Propagation in the Galaxy and in the Heliosphere: The Pathlength Distribution at Low Energy," M. Garcia-Munoz, J. A. Simpson, T. G. Guzik, J. P. Wefel, and S. H. Margolis, *Astrophysical Journal Supplement*, 64, 269 (1987).

"The Fragmentation of ^{16}O Nuclei in the Laboratory and in the Galaxy," T. G. Guzik, J. W. Mitchell, J. P. Wefel, H. J. Crawford, D. E. Grenier, J. Engelage, P. J. Lindstrom, W. Schimmerling and T. J. M. Symons, 20th ICR Conference Papers, (Moscow, USSR, 1987), Vol. 2, p. 141.

"Interstellar Propagation and the Energy Spectra of Nuclei in the Galactic Cosmic Radiation," T. G. Guzik, J. P. Wefel and J. J. Beatty, 20th ICR Conference Papers, (Moscow, USSR, 1987), Vol. 2, P. 226.

"An Overview of Cosmic Ray Research: Composition Acceleration and Propagation," John P. Wefel, in Genesis and Propagation of Cosmic Rays, eds. M. M. Shapiro and J. P. Wefel (Dordrecht, Holland, 1987; D. Reidel and Co.), p. 1.

B) Books:

Cosmic Ray and High Energy Gamma Ray Experiments for the Space Station Era, eds. W. V. Jones and J. P. Wefel, (Baton Rouge, LA, 1985, Center for Continuing Education), 569 p.

Genesis and Propagation of Cosmic Rays, eds. J. P. Wefel and M. M. Shapiro, NATO ASI Series, (Dordrecht, Holland; 1987; D. Reidel Co.), in press.

C) Unpublished Reports and Presentations:

"Implications of New Measurements of $^{16}\text{O} + p \rightarrow ^{12,13}\text{C}, ^{14,15}\text{N}$ for the Abundances of C, N Isotopes at the Cosmic Ray Source," T. G. Guzik, J. P. Wefel, H. J. Crawford, D. E. Grenier, P. J. Lindstrom, W. Schimmerling and T. J. M. Symons, Bull. Am. Phys. Soc., 30, 762 (1985).

"Galactic Propagation Models Consistent with the Cosmic Ray Lifetime Derived from ^{10}Be Measurements," J. P. Wefel, T. G. Guzik, M. Garcia-Munoz and J. A. Simpson, Bull. Am. Phys. Soc., 30, 764 (1985).

"The Energy Dependence of Secondary to Primary Ratios below 1 GeV/nucleon Including Distributed Reacceleration," T. G. Guzik, J. P. Wefel and J. J. Beatty, Bull. Am. Phys. Soc., 32, 1122 (1987).

ATTACHMENTS

1) Reprint

"Cosmic Ray Propagation in the Galaxy and in the Heliosphere:
The Path-length Distribution at Low Energy," *Astrophysical Journal
Supplement Series*, 64, 269-304 (1987).

2) Preprint

"An Overview of Cosmic Ray Research: Composition, Acceleration
and Propagation," to appear in Genesis and Propagation of Cosmic
Rays, eds. M. M. Shapiro and J. P. Wefel, D. Reidel and Co., NATO
ASI Series C. (1987).